Earth Sciences
2024, Vol. 13, No. 4, pp. 151-162
https://doi.org/10.11648/j.earth.20241304.14

Research Article

Properties of Biochar Prepared by Solar Pyrolysis and Its Adsorption of Cu^{2+} in Water

Taotao Sun[1, 2, †], Mian Muhammad Ahson Aslam[1, 2, †], Guangquan Chen[2], Yuchen Ye[1], Wentao Xu[1], Changsheng Peng[1, *]

[1]School of Chemical and Environmental Engineering, Anhui Polytechnic University, Wuhu, China

[2]Observation and Research Station of Seawater Intrusion and Soil Salinization, Laizhou Bay, Ministry of Natural Resources, Qingdao, China

Abstract

This study investigates the potential of biochar produced via a solar pyrolysis system and its effectiveness in removing copper (Cu^{2+}) ions from water, presenting a sustainable and energy-efficient method for biochar production and biomass recycling. Two common agricultural and livestock wastes, corn straw and cow dung, were used as raw materials to produce biochar. These materials underwent solar pyrolysis under limited oxygen conditions to produce biochar, which was then compared to biochar produced via traditional pyrolysis. The comparison involved elemental analyses, infrared spectroscopy, scanning electron microscopy, and specific surface area and pore size analysis to highlight differences in their physical and chemical properties. Adsorption experiments were conducted to evaluate the adsorptive capacity of biochar for copper ions (Cu^{2+}) from water, determining the optimal pH conditions and underlying adsorption mechanisms. The findings reveal that biochar produced through solar pyrolysis exhibits similar properties and Cu^{2+} adsorption capacities to those prepared by traditional methods. Specifically, cow dung biochar demonstrated a higher adsorption capacity for Cu^{2+} compared to corn straw biochar. The Cu^{2+} adsorption by corn straw biochar followed the Langmuir isothermal adsorption model and pseudo-second-order kinetic equation, whereas cow dung biochar conformed to the Freundlich isothermal adsorption model and pseudo-second-order kinetic equation. By demonstrating the comparable efficacy of solar pyrolysis biochar in heavy metal adsorption, this study highlights its potential for sustainable environmental remediation and biomass utilization.

Keywords

Biochar, Solar Pyrolysis, Wastewater Treatment, Copper Pollution, Adsorptive Removal

1. Introduction

With the development of industrialization, industries such as mining, electroplating, and metal processing generate substantial amounts of acidic wastewater annually [1]. The concentration of copper ions in each liter of wastewater can range from dozens to hundreds of milligrams, posing serious pollution problems if untreated wastewater is discharged into natural

*Corresponding author: pcs2208@mail.ahpu.edu.cn (Changsheng Peng)

† Taotao Sun and Mian Muhammad Ahson Aslam are co-first authors.

Received: 9 July 2024; **Accepted:** 14 August 2024; **Published:** 20 August 2024

water bodies [2, 3]. Free Cu^{2+} in natural water is widely considered toxic to aquatic organisms. While trace amounts of copper are essential for life, excessive copper is harmful to humans, animals, and plants. It leads to ecological imbalances, copper poisoning in aquatic organisms, and the bioaccumulation of high copper concentrations in the food chain, ultimately affecting human safety [4]. To control copper pollution, China has set the maximum allowable discharge concentration of copper and its compounds in industrial wastewater at 1 mg/L.

Adsorption is an effective method for treating heavy metal wastewater [5]. Biochar is considered a green, environmentally friendly adsorbent due to its porous structure, large specific surface area, and abundant functional groups on the surface [6, 7]. These characteristics enable biochar to effectively remove toxic metal ions and other contaminants from water, with its raw materials being widely and cheaply sourced [8]. The specific surface area, pore size distribution, ion exchange capacity, and molecular composition of biochar are primarily associated with the pyrolysis parameters used in its preparation. These parameters include pyrolysis temperature, pyrolysis time, and heat transfer rate. Different pyrolysis process parameters yield biochar with varying properties [9].

Biochar used in water treatment is typically prepared through slow pyrolysis, which produces biochar with a larger specific surface area and better-developed pore structure, facilitating contaminants. Traditional pyrolysis technology relies on electric heating to provide the necessary heat for the biomass pyrolysis process, leading to high energy consumption, high pollution, and increased production costs. These factors hinder the widespread application of biochar as an adsorbent material [10, 11].

Solar pyrolysis technology uses biomass as the reactant and solar energy to provide heat during the high-temperature pyrolysis reaction. Compared to traditional pyrolysis technology, solar pyrolysis reduces energy consumption and environmental pollution, making it a novel technology for energy conservation and environmental protection [12]. However, there are few studies on the preparation of biochar by solar pyrolysis, with most research focusing on the use of biochar as a biofuel rather than its application in environmental remediation.

This study aims to use solar energy for the pyrolysis of corn straw and cow dung to prepare biochar, comparing it with biochar produced by traditional methods. A series of physicochemical methods are used to analyze the properties of biochar prepared by solar pyrolysis and compare them to biochar prepared using a traditional tube furnace. Additionally, the adsorptive capacity of biochar for heavy metal ions, particularly Cu^{2+}, from water is evaluated. Factors such as the initial concentration of Cu^{2+}, contact time, and solution pH are investigated to understand their impact on adsorption behavior and mechanism. Isothermal adsorption models are used to characterize the adsorption process, and the experimental data are kinetically validated. Additionally, the effect of pH on the surface charge distribution of biochar and the presence of heavy metal ions is discussed.

Finally, this study verifies the feasibility of solar pyrolysis in biochar preparation, understands the adsorption mechanism of Cu^{2+} by corn straw and cow dung biochar, and provides new insights for the production of energy-saving and environmentally friendly biochar and the utilization of biomass waste.

2. Methodology

2.1. Solar Pyrolysis System

We designed and constructed a solar pyrolysis system integrating a concentrated radiation system with a thermochemical biomass conversion system. This system comprises three main components: a solar concentrator, a tubular reactor, and a solar tracking system (Figure 1). The trough parabolic concentrator, coated with a silver-mirror surface, focuses solar radiation in a straight line. The reactor, consisting of an evacuated collector tube, absorbs solar radiation and converts it into heat energy.

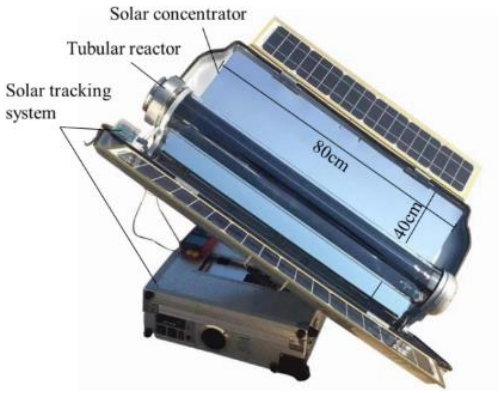

Figure 1. *Solar pyrolysis device.*

2.2. The Preparation of Biochar

The raw materials used were corn straw and cow dung. Corn straw was collected from farmland in Heze, Shandong province, and cow dung from a farm in Zhoukou, Henan province. Elemental analyses of these materials are presented in Table 1. Both raw materials were rinsed several times with distilled water, oven-dried at 105 ℃ (Electrothermal blowing dry box, DHG-9023A, Shanghai Jinghong) until constant weight, and crushed to 35 mesh size. Subsequently, they underwent to pyrolysis for 2 hours at 450 ℃ using solar pyrolysis installation (Photovoltaic heat pipe combination, HGC-0.8/6.5 Kz, Shandong Huangmin) and a tube furnace (Tubular furnace atmosphere, SLG1200-60, Shanghai). After cooling to room temperature, the biochar was stored in a desiccator. The biochar from solar pyrolysis was labeled SJ450 (corn stalk) and SN450 (cow dung), while biochar from the tubular furnace was labeled CJ450 and CN450, respectively.

Table 1. Proximate analysis and elemental analysis of raw materials.

Analysis item	Proximate analysis (wt.% db)			Elemental analysis (wt.% db)				Produce area
	FC	A	VM	C	H	O	N	
Corn stalk	20.7	4.67	71.54	44.02	5.82	43.65	1.52	*Heze, Shangdong*
Cow dung	13.9	36.4	49	33.17	2.80	25.28	2.31	*Zhoukou, Henan*

Note: FC, A and VM refer to fixed carbon, ash and volatile content respectively, and db is oven-dry basis.

2.3. The Characterization of Biochar

We determined the biochar composition, including carbon (C), oxygen (O), hydrogen (H), and nitrogen (N) content, using an Element analyzer (Elementar Vario EL Cube, Hanau, Germany). Industrial analysis followed the ASTM D 3172 standard, quantifying volatile matter, fixed carbon, and ash content. The volatile matter was measured by weight loss after heating at 950 ℃ for 10 minutes, while ash content was determined after 6 hours at 750 ℃. The fixed carbon was calculated by subtracting the volatile matter and ash from the total mass.

For morphological characterization, we used a field emission scanning electron microscope (SU8200, HITACHI, Japan) to observe surface morphology and structure. The specific surface area and pore diameter were measured using the Brunner-Emmet-Teller method and an N_2 adsorption apparatus (ASAP2460, Micromeritics, USA). Functional groups on the biochar surface were analyzed using a Fourier infrared spectrometer (FT-IR TENSOR 27, Bruker, USA).

2.4. Adsorption of Cu^{2+} by Biochar

We conducted batch equilibrium experiments to assess the adsorptive capacity of biochar for Cu^{2+} ions. A solution of $Cu(NO_3)_2$ $3H_2O$ was prepared at various concentrations. Corn straw and cow dung biochar samples (0.1000 g - 0.0005 g) were added to these solutions, with 0.01 mol/L $NaNO_3$ as the background electrolyte. Each experimental setup included parallel blank tests using distilled water (biochar + H_2O). The concentration of Cu^{2+} in the solutions was determined using inductively coupled plasma mass spectrometry (ICP-MS Nexlon 350X, PerkinElmer).

2.4.1. Effect of pH on Adsorption

Weighed biochar samples were placed in 100 mL conical flasks containing 100 mL of 50 mg/L Cu^{2+} solution, with 0.1 mol/L $NaNO_3$ as the background electrolyte. The pH was adjusted to 1, 2, 3, 4, 5, and 6 using 0.1 mol/L NaOH and HNO_3 solutions. The reaction solution in the flasks were stirred at 150 r/min for 24 hours at 25±3 ℃, then centrifuged at 4000 r/min for 10 minutes. The supernatant was filtered to determine the Cu^{2+} concentration. The adsorption capacity (q_e, mg/g) of biochar for Cu^{2+} was calculated using Equation (1).

$$q_e = \frac{(c_0 - c_e)V}{m} \quad (1)$$

where c_0 and c_e are the initial and equilibrium concentrations of Cu^{2+} (mg/L), V is the solution volume (L), and m is the mass biochar used (g).

2.4.2. Adsorption Isothermal Test

Cu^{2+} solutions with concentrations of 20, 40, 80, 120, 150, and 200 mg/L were prepared. The solutions were stirred at 150 rpm for 24 hours at 25 ℃, followed by centrifugation and filtration to determine the Cu^{2+} concentration. The adsorption isotherms for the uptake of Cu^{2+} at 25 ℃ for the two types of biochar were fitted using the Langmuir and Freundlich models, as described in Equations (2) and (3).

$$\frac{C_e}{q_e} = \frac{1}{b * q_m} + C_e / q_m \quad (2)$$

$$ln\, q_e = ln\, K_f + \frac{1}{n} * ln\, C_e \quad (3)$$

where C_e is the equilibrium concentration of Cu^{2+}, q_e is the adsorption capacity at equilibrium (mg/g), b is the affinity constant, q_m is the maximum adsorption capacity, K_f is the Freundlich constant (mg/g), and n is the adsorption intensity.

2.4.3. Adsorption Kinetics Test

A 100 mL solution with initial Cu^{2+} concentration of 50 mg/L was used, with samples taken at various time intervals (15, 30, 60, 120, 240, 480, 960, 1440, 2880 min) at 25±3 ℃ and 150 r/min for 24 h. The adsorption kinetics were analyzed using pseudo-first-order (Equation 4), pseudo-second-order (Equation 5), and intra-particle diffusion (Equation 6) to compare the adsorption rates and mechanisms of the two biochar types.

$$q_t = q_e(1 - e^{-k_1 t}) \quad (4)$$

$$\frac{t}{q_t} = \frac{1}{k_2 q_e^2} + \frac{t}{q_e} \quad (5)$$

$$q_t = k_{ip} t^{1/2} + C \quad (6)$$

where q_t is the amount of metal ions adsorbed at time t (mg/g), q_e is the amount of metal ions adsorbed at equilibrium (mg/g), k_1 is the pseudo-first-order rate constant (L/min), k_2 is the pseudo-second-order rate constant ($g \cdot mg^{-1} \cdot min^{-1}$), and K_{ip} is the intraparticle constant（mg (g ·$min^{0.5}$)$^{-1}$).

3. Result and Discussion

3.1. Thermogravimetric Analysis of Biomass

To determine the optimal temperature conditions for biomass pyrolysis to produce biochar, we conducted thermogravimetric and differential thermogravimetric analyses on corn stalks and cow dung. Biomass typically contains cellulose, hemicellulose, and lignin, each exhibiting distinct pyrolysis characteristics. Hemicellulose primarily decomposes between 210 ℃ and 370 ℃, cellulose between 260 ℃ and 410 ℃, and lignin within a broader range of 200 ℃ to 600 ℃. The relatively stable structure of lignin results in carbon-based solid products post-pyrolysis, with the remaining solid mass stabilizing after temperatures exceed 400 ℃ [13]. Corn stalks comprise cellulose, hemicellulose, and lignin [14], while cow dung mainly consists of undigested lignin and cellulose [15].

As illustrated in Figure 2, the pyrolysis process for both materials can be divided into three distinct stages. The first stage is the dehydration and drying phase (30-130 ℃), characterized by a single weight loss peak due to the evaporation of water and minor volatile substances. The second stage, occurring between 210 ℃ and 410 ℃, is the main pyrolysis phase, where significant degradation of organic matter, such as cellulose and hemicellulose, takes place. During this phase, corn straw exhibit a weight loss of approximately 70%, while cow dung shows a weight loss of about 35%. According to the differential thermogravimetric (DTG) curve, the maximum weight loss rate for corn straw occurs at 330 ℃, and for cow dung, it occurs at 310 ℃. The final stage is the carbonization phase, occurring above 450 ℃, where the raw materials undergo further pyrolysis with minimal heat loss, resulting in approximately 10% weight loss. During this stage, the carbon and ash content in the solid biochar increase. The high ash content and low volatile content in cow dung contribute to its higher residual mass post-pyrolysis.

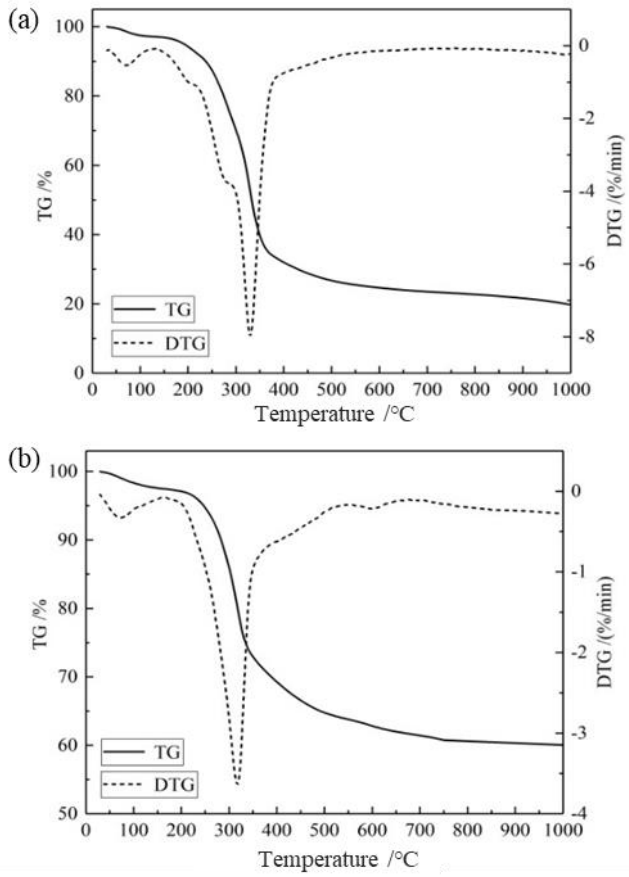

Figure 2. *TG and DTG analysis of biomass material: (a) corn straw, (b) cow dung.*

3.2. SEM Analysis

Scanning electron microscopy (SEM) images reveal significant differences in the surface morphology of biochar prepared from corn straw and cow dung at 450 ℃ (Figure 3). The surface morphology of biochar produced from different raw materials at the same pyrolysis temperature varies considerably. Biochar derived from corn straw exhibits a porous structure, primarily due to the different decomposition temperatures of its cellulose, hemicellulose, and lignin components. These components decompose and release volatile gases, creating a porous surface morphology [16]. In contrast, cow dung biochar displays a granular structure, largely due to ash accumulation, and features relatively undeveloped pore structures [17].

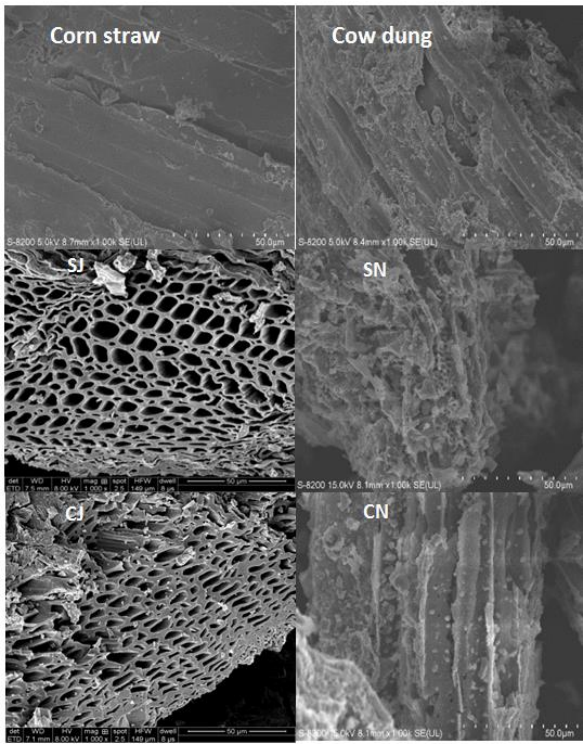

Figure 3. *SEM images of biomass before and after different pyrolysis processes.*

3.3. FTIR Characteristics

Fourier-transform infrared spectroscopy (FTIR) was employed to evaluate the impact of different pyrolysis methods and raw materials on the functional groups present on the surface of biochar. The characterization tests conducted on samples before and after pyrolysis revealed that the functional groups in biochar are similar across different preparation methods. The results, shown in Figure 4, indicate that the characteristic absorption peaks of the samples remain largely consistent, suggesting that the functional groups contained within the biochar are similar. Additionally, the amplitude of absorption peak vibrations in biochar produced by different methods is relatively comparable, indicating minimal differences in functional group content.

Several key changes were observed:

1) The absorption peak at a wave number of 3400 cm^{-1}, associated with the O-H stretching vibration of water molecules, disappears after pyrolysis due to water dispersion during the process [18].

2) The absorption peak at 2918-2925 cm^{-1}, attributed to the C-H stretching vibration of aliphatic carbon chains in cellulose and other polymers, significantly decreases in corn straw biochar and disappears in cow dung biochar post-pyrolysis.

3) The absorption peak at 1637-1648 cm^{-1}, corresponding to the C=O stretching vibration, and the peak at 1418-1421 cm^{-1}, related to aromatic carbon C=C stretching vibration [19], both decrease in intensity post-pyrolysis. This suggests the decomposition of carboxyl, carbonyl, and ester groups, with corn straw biochar showing increased aromatization and cow dung biochar displaying accumulation of mineral components.

4) The absorption peak at 1043-1045 cm^{-1}, primarily generated by C-O-C and C-H bond stretching vibrations, significantly weakens after the pyrolysis of corn straw [20].

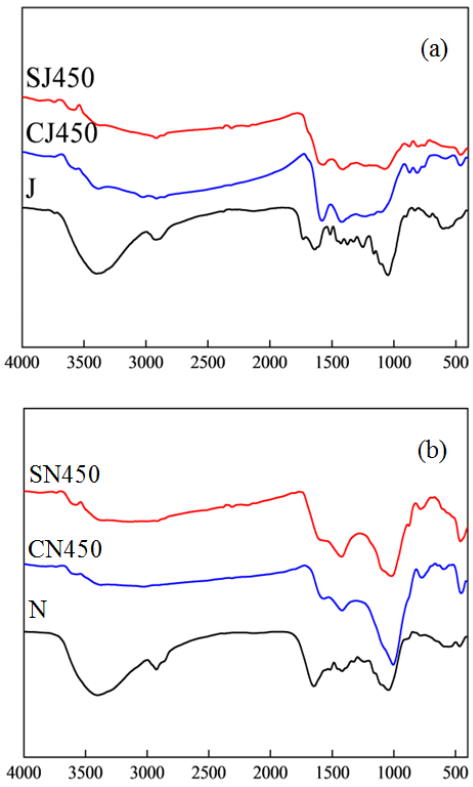

Figure 4. *FTIR spectra of corn straw (a) and cow dung (b) and their corresponding biochar.*

3.4. BET Analysis

To further compare the structural characteristics of biochar produced by solar pyrolysis and traditional pyrolysis, we used the Brunauer-Emmett-Teller (BET) method to analyze the specific surface area and pore diameter of the biochar. Table 2 presents the data on the pore characteristics of biochar prepared by both methods, including specific surface area, total pore volume, and average pore diameter. The results show minimal differences in the pore characteristics of biochar produced by solar pyrolysis compared to traditional methods [21-23]. However, significant differences are observed in the pore structures of biochar derived from different raw materials.

Biochar produced from corn straw has a significantly higher specific surface area and total pore volume than biochar produced from cow cow dung, with a smaller average pore diameter. This indicates a more developed pore structure in corn straw biochar, consistent with the SEM results. The continuous escape of volatiles generated by the decom-

position of cellulose, hemicellulose, and other substances in corn straw during pyrolysis leads to an increase in the number of internal pores and, consequently, a larger specific surface area. In contrast, cow dung contains a higher content of inorganic minerals, which negatively correlate with specific surface area. The melting of these minerals at high temperatures fills the pores in the biochar, resulting in a loss of specific surface area [24].

Table 2. *Pore structures and yields of biochar.*

Samples	S_{BET} (m^2/g)	V_{total} (mL/g)	Average pore size (nm)	Agricultural productivity (%)
SJ	29.4454	0.046928	6.1463	32.8
CJ	30.7176	0.069178	7.3343	30.8
SN	8.3480	0.0226	8.8208	57.7
CN	10.7157	0.0214	8.0954	56.7

3.5. Effect of pH on Adsorption of Cu^{2+}

To investigate the effect of initial pH on the adsorption of Cu^{2+} by biochar, we conducted adsorption experiments with Cu^{2+} solutions at pH values ranging from 1.0 to 6.0. Figure 5 shows that the initial pH significantly impacts the adsorption of Cu^{2+} by biochar. The adsorption capacity of both types of biochar increased as the pH ranged from 1.0 to 6.0. The difference in Cu^{2+} adsorption between the two biochars under varying pH conditions was minimal. However, the adsorption capacity of corn straw biochar changed more significantly between pH 1 and 4, while cow dung biochar showed a gradual increase in adsorption capacity above pH 3.

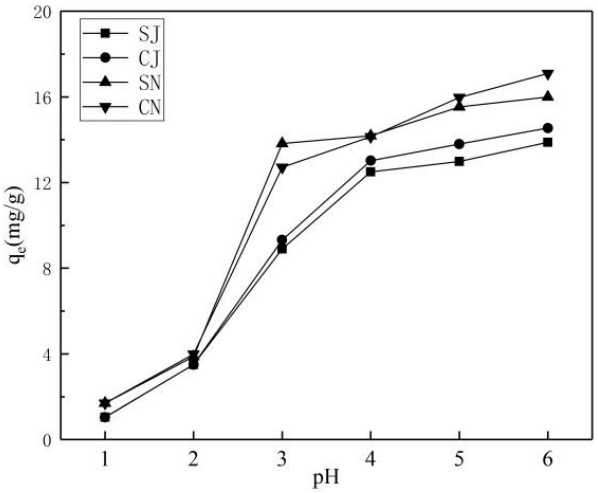

Figure 5. *Effect of solution pH on adsorption effect.*

The influence of pH on adsorption is primarily due to its effect on the surface properties of biochar and the chemical form of metal ions in solution [25]. At pH values below 5, Cu^{2+} is the predominant species. Lower pH results in higher H^+ concentrations, leading to competition between H^+ and Cu^{2+} for binding sites on the biochar surface, thereby reducing adsorption capacity. At pH values of 5 and above, $Cu(OH)^+$ becomes the dominant species. As pH increases, H^+ concentration decreases, and the biochar surface becomes increasingly electronegative, enhancing electrostatic attraction to $Cu(OH)^+$. When pH continues to rise, $Cu(OH)_2$ forms, and Cu^{2+} is gradually converted into insoluble hydroxide precipitates, favoring the adsorption of Cu^{2+} by both corn straw and cow dung biochar.

3.6. Adsorption Isotherm

Adsorption experiments were conducted to obtain isothermal adsorption properties of biochar for Cu^{2+} under different initial concentrations. As shown in Figure 6, the adsorption capacity of biochar for Cu^{2+} increased rapidly with the initial concentration, then stabilized. Biochar prepared by solar pyrolysis showed similar adsorption effects for Cu^{2+} compared to biochar produced by traditional pyrolysis methods.

To evaluate the maximum adsorption capacities of the biochars for Cu^{2+}, and to further analyze the adsorption characteristics, the Langmuir and Freundlich models were used to fit the experimental data. The fitting results are presented in Table 3. For corn straw biochar (SJ and CJ), the Langmuir model exhibited a higher correlation coefficient ($R^2 > 0.95$) than the Freundlich model, with maximum adsorption capacities of 13.52 mg/g and 14.30 mg/g, respectively. The parameter n, which indicates the affinity of biochar binding sites, was higher for CJ than SJ (n = 8.16 and 6.92, respectively), suggesting that CJ has a higher affinity Cu^{2+}, with monolayer adsorption being predominant.

For cow dung biochar (SN and CN), the Freundlich model showed a higher correlation coefficient ($R^2 > 0.98$) than the Langmuir model, indicating that Cu^{2+} adsorption mainly occurs via multilayer adsorption. The Freundlich n values for SN and CN were 4.64 and 5.90, respectively, both greater than 1, indicating strong interactions between the adsorbent and metal ions. The adsorption capacity of cow dung biochar for Cu^{2+} was better than that of corn straw biochar. Additionally, Table 4 compares the Cu^{2+} removal efficiencies of biochar's derived from corn straw and cow dung via solar pyrolysis with various other biochar's reported in the literature. The superior maximum removal capacities observed for corn straw and cow dung biochar's highlight their potential for practical applications in environmental remediation.

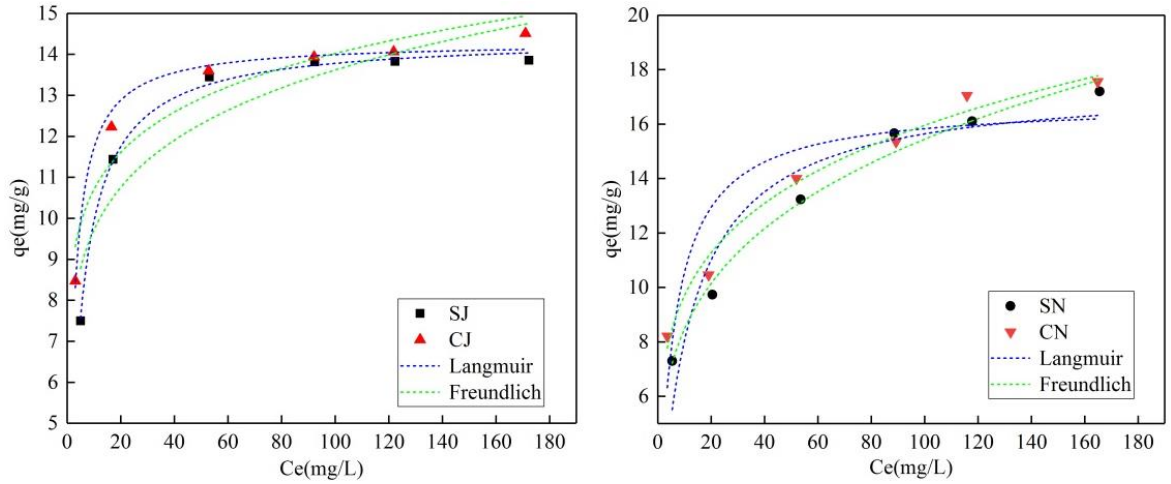

Figure 6. *Adsorption isotherms of Cu^{2+} on biochars.*

Table 3. *Best-fit parameters for isotherm models of Cu^{2+} sorption onto biochars.*

Biochar	Adsorption isotherm	Parameter1	Parameter2	R^2
SJ	Langmuir	q_m=13.52	K=0.22	0.996
	Freundlich	n=6.92	K_f=0.15	0.858
CJ	Langmuir	q_m=14.30	K=0.45	0.959
	Freundlich	n=8.16	K_f=0.12	0.898
SN	Langmuir	q_m=17.48	K=0.09	0.884
	Freundlich	n=4.64	K_f=0.26	0.985
CN	Langmuir	q_m=17.77	K=0.17	0.76
	Freundlich	n=5.90	K_f=0.22	0.980

Table 4. *Compares the Cu^{2+} removal efficiencies of biochar's derived from corn straw and cow dung via solar pyrolysis with various other biochar's reported in the literature.*

Biomass for biochar	Pyrolysis Conditions		Adsorption capacity (mg/g)	Reference
	Temperature (℃)	Time (min)		
Corn straw	600	120	12.5	[26]
Hardwood	450	120	6.8	
Scots pine	700	45	1.9	[27]
Pine sawdust	550	120	3.0	[28]
Tea waste+Sewage sludge	300	120	16.4	[29]
Switchgrass	300^{HTC}	30	4.0	[30]
Pig manure	400	120	12.72	[31]
Pig manure	700	120	9.1	
pinewood sawdust	700	120	8.9	[32]
Softwood (Pine)	700	30	1.47	[33]

Biomass for biochar	Pyrolysis Conditions		Adsorption capacity (mg/g)	Reference
	Temperature (℃)	Time (min)		
Hardwood (Jarrah)			4.4	
Sawdust	500	-	3.02 (as prepared) 15.1 (Amino modified)	[34]
Corn Straw	450	120	17.5	This study
Cow Dung			17.8	

3.7. Adsorption Kinetics

Figure 7 shows that the biochar produced via two different pyrolysis methods exhibited different Cu^{2+} adsorption capacities at an initial concentration of 50 mg/L. More than 80% of the total adsorption occurred within the first 8 hours, with the rate of adsorption gradually decreasing until equilibrium was reached. This initial rapid adsorption can be attributed to the abundant pores and surface functional groups on biochar, which provide numerous binding sites for Cu^{2+} ions. Over time, the number of active binding sites diminishes, and electrostatic repulsion between ions increases [35], slowing down the adsorption process until equilibrium is achieved [36].

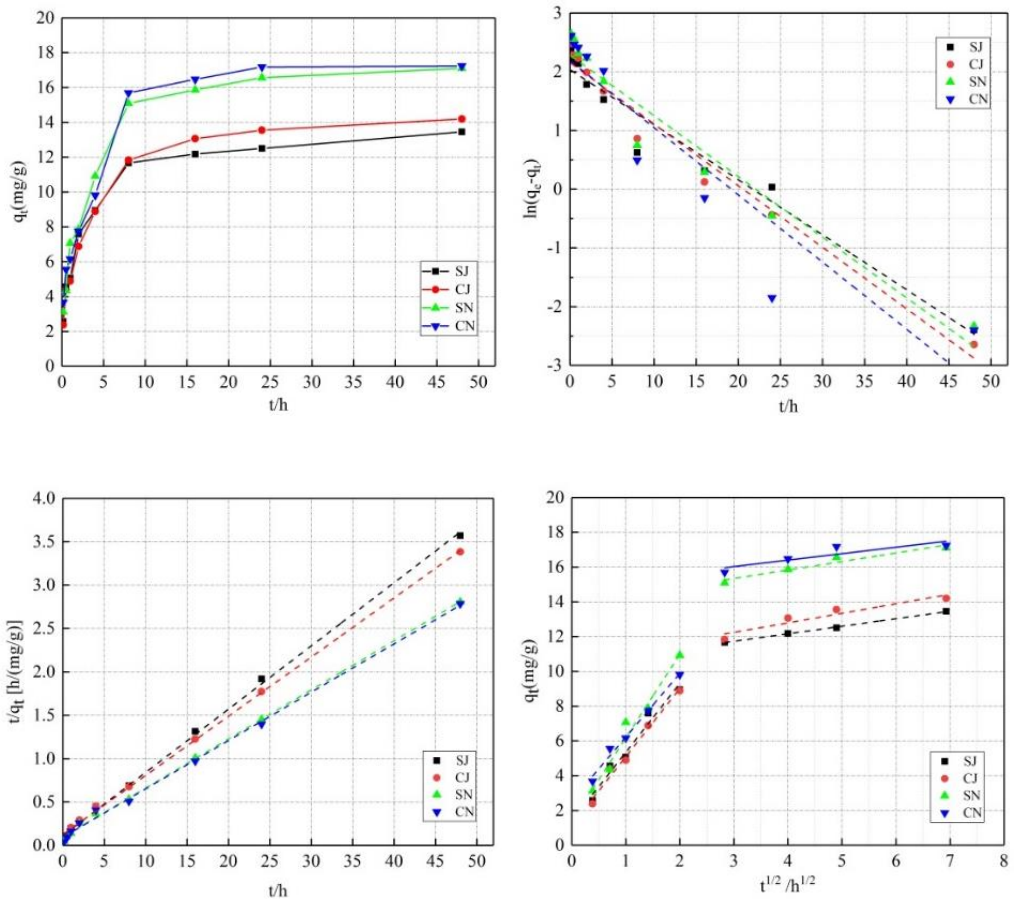

Figure 7. *Kinetic data and fitting model of adsorption of Cu^{2+} by biochar in aqueous solution.*

To analyze the adsorption rate changes, we applied pseudo first- and second-order kinetics, and intra-particle diffusion equations to the experimental data. Table 5 shows that the pseudo second-order kinetic equation provided a better fit for

the adsorption data of Cu^{2+} by all four types of biochar compared to the pseudo first-order kinetic and intra-particle diffusion equations. The second-order kinetic model effectively describes the entire adsorption process, including external liquid film diffusion, internal particle diffusion, and surface adsorption, offering a comprehensive view of the kinetic mechanism. The diffusion equation fitting indicated a faster initial rate of Cu^{2+} ion diffusion to the biochar surface, which significantly slowed down as the copper ion concentration decreased. As for the intra-particle diffusion model, fitted line did not pass through the origin, it suggests that intra-particle diffusion is not the sole rate-controlling step; other processes also influence the adsorption reaction rate [37].

Table 5. *Fitting data of four kinetic models of adsorption of Cu^{2+} by biochar.*

Biochar	pseudo-first order			pseudo-second order			intra-particle diffusion		
	k_1	q_e	R^2	k_2	q_e	R^2	k_{ip}	C	R^2
SJ	0.094	13.54	0.9513	0.048	13.72	0.9985	3.963	1.375	0.9562
CJ	0.105	14.19	0.9714	0.038	14.65	0.9986	3.927	1.154	0.9794
SN	1.103	17.20	0.9452	0.037	17.68	0.9986	4.810	1.365	0.9622
CN	0.114	17.33	0.8525	0.033	17.96	0.9967	3.665	2.554	0.9836

4. Conclusion

In this study, biochar was produced from two different biomass materials using two pyrolysis methods. Under identical pyrolysis conditions, cow dung biochar (SN, CN) demonstrated a stronger ability to remove Cu^{2+} from aqueous solutions compared to corn straw biochar (SJ, CJ). The adsorption of Cu^{2+} by cow dung biochar aligned more with the Freundlich model, indicating primarily multilayer adsorption. Conversely, the Cu^{2+} adsorption by corn straw biochar better fit the Langmuir model suggesting monolayer adsorption.

The adsorption kinetics data revealed two stages in the adsorption process: a fast initial reaction followed by a slower phase. The initial stage, dominated by Cu^{2+} diffusion, reached equilibrium quickly. The pseudo-second-order kinetic model best described the adsorption kinetics of all four biochar types, indicating that the adsorption rate is primarily controlled by chemical adsorption.

Comparing the two pyrolysis methods, biochar produced via solar pyrolysis (SJ, SN) had slightly lower Cu^{2+} adsorption performance than biochar produced via traditional pyrolysis (CJ, CN). However, solar pyrolysis offers economic and environmental benefits, such as not consuming fossil fuels or producing additional pollution, which makes it a cost-effective and sustainable technology for biomass pyrolysis. This method holds promise for future applications in water treatment, offering advantages in energy conservation and environmental protection.

Abbreviations

J	Corn Stalk
N	Cow Dung
SJ	Solar Pyrolysis of Corn Stalk
SN	Solar Pyrolysis of Cow Dung
CJ	Tube Furnace Pyrolysis of Corn Stalk
CN	Tube Furnace Pyrolysis of Cow Dung

Acknowledgements

This work was supported by the Anhui Polytechnic University Startup Foundation for Introduced Talents, China (2022YQQ076), the Key R&D and Achievement Transformation Projects of Wuhu Science and Technology Plan (2023yf102) and the Open Research Fund of Observation and Research Station of Seawater Intrusion and Soil Salinization, Laizhou Bay, Ministry of Natural Resources (2024LZORS002).

Author Contributions

Taotao Sun: Data curation, Methodology, Formal Analysis, Writing – original draft

Mian Muhammud Ahson Aslam: Formal Analysis, Validation, Investigation, Writing – review & editing, Funding acquisition, Project administration

Guangquan Chen: Formal Analysis, Investigation, Writing – review & editing

Yuchen Ye: Data curation, Visualization

Wentao Xu: Data curation, Visualization

Changsheng Peng: Conceptualization, Formal Analysis, Investigation, Resources, Supervision, Writing – review & editing, Funding acquisition, Project administration

Data Availability Statement

The data supporting the outcome of this research work has been reported in this manuscript.

Conflicts of Interest

The authors declare no conflicts of interest.

References

[1] XIE S, YU C, PENG B, et al. A re-assessment of metal pollution in the Dexing mining area in Jiangxi province, China: current status, hydro-geochemical controls, and effectiveness of remediation practices [J]. International Journal of Environmental Science and Technology, 2022, 19(11): 10707-10722. https://doi.org/10.1007/s13762-021-03887-x

[2] DEHGHANI M H, OMRANI G A, KARRI R R. Chapter 11 - Solid Waste—Sources, Toxicity, and Their Consequences to Human Health [M]//KARRI R R, RAVINDRAN G, DEHGHANI M H. Soft Computing Techniques in Solid Waste and Wastewater Management. Elsevier. 2021: 205-213. https://doi.org/10.1016/B978-0-12-824463-0.00013-6

[3] EL-NEMR M A, AIGBE U O, HASSAAN M A, et al. The use of biochar-NH2 produced from watermelon peels as a natural adsorbent for the removal of Cu(II) ion from water [J]. Biomass Conversion and Biorefinery, 2024, 14(2): 1975-1991. https://doi.org/10.1007/s13399-022-02327-1

[4] NICOLAOU E, PHILIPPOU K, ANASTOPOULOS I, et al. Copper Adsorption by Magnetized Pine-Needle Biochar [J/OL] 2019, 7(12). https://doi.org/10.3390/pr7120903

[5] SUDARNI D H A, AIGBE U O, UKHUREBOR K E, et al. Malachite Green Removal by Activated Potassium Hydroxide Clove Leaf Agrowaste Biosorbent: Characterization, Kinetic, Isotherm, and Thermodynamic Studies [J]. Adsorption Science & Technology, 2021, 2021: 1145312. https://doi.org/10.1155/2021/1145312

[6] WANG J, WANG S. Preparation, modification and environmental application of biochar: A review [J]. Journal of Cleaner Production, 2019, 227: 1002-1022. https://doi.org/10.1016/j.jclepro.2019.04.282

[7] ZHOU S, YANG Y-X, CAO J-J, et al. Monitoring of copper adsorption on biochar using spectral induced polarization method [J]. Environmental Research, 2024, 251: 118778. https://doi.org/10.1016/j.envres.2024.118778

[8] AHMAD M, RAJAPAKSHA A U, LIM J E, et al. Biochar as a sorbent for contaminant management in soil and water: A review [J]. Chemosphere, 2014, 99: 19-33. https://doi.org/10.1016/j.chemosphere.2013.10.071

[9] TRAZZI P A, LEAHY J J, HAYES M H B, et al. Adsorption and desorption of phosphate on biochars [J]. Journal of Environmental Chemical Engineering, 2016, 4(1): 37-46. https://doi.org/10.1016/j.jece.2015.11.005

[10] MANY à J J. Pyrolysis for Biochar Purposes: A Review to Establish Current Knowledge Gaps and Research Needs [J]. Environmental Science & Technology, 2012, 46(15): 7939-7954. https://doi.org/10.1021/es301029g

[11] ROBERTS K G, GLOY B A, JOSEPH S, et al. Life Cycle Assessment of Biochar Systems: Estimating the Energetic, Economic, and Climate Change Potential [J]. Environmental Science & Technology, 2010, 44(2): 827-833. https://doi.org/10.1021/es902266r

[12] ZENG K, GAUTHIER D, SORIA J, et al. Solar pyrolysis of carbonaceous feedstocks: A review [J]. Solar Energy, 2017, 156: 73-92. https://doi.org/10.1016/j.solener.2017.05.033

[13] QUAN C, GAO N, SONG Q. Pyrolysis of biomass components in a TGA and a fixed-bed reactor: Thermochemical behaviors, kinetics, and product characterization [J]. Journal of Analytical and Applied Pyrolysis, 2016, 121: 84-92. https://doi.org/10.1016/j.jaap.2016.07.005

[14] HU M, ZHU G, CHEN Y, et al. Enhanced co-pyrolysis of corn stalk and bio-tar into phenolic-rich biooil: Kinetic analysis and product distributions [J]. Journal of Analytical and Applied Pyrolysis, 2024, 177: 106358. https://doi.org/10.1016/j.jaap.2024.106358

[15] ZHANG D, SUN Z, FU H, et al. Upgrading of cow manure by hydrothermal carbonization: Evaluation of fuel properties, combustion behaviors and kinetics [J]. Renewable Energy, 2024, 225: 120269. https://doi.org/10.1016/j.renene.2024.120269

[16] ZHANG C, ZHANG Z, ZHANG L, et al. Evolution of the functionalities and structures of biochar in pyrolysis of poplar in a wide temperature range [J]. Bioresource technology, 2020, 304: 123002. https://doi.org/10.1016/j.biortech.2020.123002

[17] ZHANG P, ZHANG X, YUAN X, et al. Characteristics, adsorption behaviors, Cu(II) adsorption mechanisms by cow manure biochar derived at various pyrolysis temperatures [J]. Bioresource Technology, 2021, 331: 125013. https://doi.org/10.1016/j.biortech.2021.125013

[18] WANG Z, ZHENG H, LUO Y, et al. Characterization and influence of biochars on nitrous oxide emission from agricultural soil [J]. Environmental Pollution, 2013, 174: 289-296. https://doi.org/10.1016/j.envpol.2012.12.003

[19] ZHU D, KWON S, PIGNATELLO J J. Adsorption of Single-Ring Organic Compounds to Wood Charcoals Prepared under Different Thermochemical Conditions [J]. Environmental Science & Technology, 2005, 39(11): 3990-3998. https://doi.org/10.1021/es050129e

[20] PETERSON S C, JACKSON M A. Simplifying pyrolysis: Using gasification to produce corn stover and wheat straw biochar for sorptive and horticultural media [J]. Industrial Crops and Products, 2014, 53: 228-235. https://doi.org/10.1016/j.indcrop.2013.12.028

[21] PARIYAR P, KUMARI K, JAIN M K, et al. Evaluation of change in biochar properties derived from different feedstock and pyrolysis temperature for environmental and agricultural application [J]. Science of The Total Environment, 2020, 713: 136433. https://doi.org/10.1016/j.scitotenv.2019.136433

[22] TURUNEN M, HYVäLUOMA J, HEIKKINEN J, et al. Quantifying the pore structure of different biochars and their impacts on the water retention properties of Sphagnum moss growing media [J]. Biosystems Engineering, 2020, 191: 96-106. https://doi.org/10.1016/j.biosystemseng.2020.01.006

[23] KIM K H, KIM J-Y, CHO T-S, et al. Influence of pyrolysis temperature on physicochemical properties of biochar obtained from the fast pyrolysis of pitch pine (Pinus rigida) [J]. Bioresource Technology, 2012, 118: 158-162. https://doi.org/10.1016/j.biortech.2012.04.094

[24] CHEN G, WANG C, TIAN J, et al. Investigation on cadmium ions removal from water by different raw materials-derived biochars [J]. Journal of Water Process Engineering, 2020, 35: 101223. https://doi.org/10.1016/j.jwpe.2020.101223

[25] CHUN Y, SHENG G, CHIOU C T, et al. Compositions and Sorptive Properties of Crop Residue-Derived Chars [J]. Environmental Science & Technology, 2004, 38(17): 4649-4655. https://doi.org/10.1021/es035034w

[26] CHEN X, CHEN G, CHEN L, et al. Adsorption of copper and zinc by biochars produced from pyrolysis of hardwood and corn straw in aqueous solution [J]. Bioresource Technology, 2011, 102(19): 8877-8884. https://doi.org/10.1016/j.biortech.2011.06.078

[27] KOMKIENE J, BALTRENAITE E. Biochar as adsorbent for removal of heavy metal ions [Cadmium(II), Copper(II), Lead(II), Zinc(II)] from aqueous phase [J]. International Journal of Environmental Science and Technology, 2016, 13(2): 471-482. https://doi.org/10.1007/s13762-015-0873-3

[28] LOU K, RAJAPAKSHA A U, OK Y S, et al. Sorption of copper(II) from synthetic oil sands process-affected water (OSPW) by pine sawdust biochars: effects of pyrolysis temperature and steam activation [J]. Journal of Soils and Sediments, 2016, 16(8): 2081-2089. https://doi.org/10.1007/s11368-016-1382-9

[29] FAN S, LI H, WANG Y, et al. Cadmium removal from aqueous solution by biochar obtained by co-pyrolysis of sewage sludge with tea waste [J]. Research on Chemical Intermediates, 2018, 44(1): 135-154. https://doi.org/10.1007/s11164-017-3094-1

[30] REGMI P, GARCIA MOSCOSO J L, KUMAR S, et al. Removal of copper and cadmium from aqueous solution using switchgrass biochar produced via hydrothermal carbonization process [J]. Journal of Environmental Management, 2012, 109: 61-69. https://doi.org/10.1016/j.jenvman.2012.04.047

[31] MENG J, FENG X, DAI Z, et al. Adsorption characteristics of Cu(II) from aqueous solution onto biochar derived from swine manure [J]. Environmental Science and Pollution Research, 2014, 21(11): 7035-7046. https://doi.org/10.1007/s11356-014-2627-z

[32] POO K-M, SON E-B, CHANG J-S, et al. Biochars derived from wasted marine macro-algae (Saccharina japonica and Sargassum fusiforme) and their potential for heavy metal removal in aqueous solution [J]. Journal of Environmental Management, 2018, 206: 364-372. https://doi.org/10.1016/j.jenvman.2017.10.056

[33] JIANG S, HUANG L, NGUYEN T A H, et al. Copper and zinc adsorption by softwood and hardwood biochars under elevated sulphate-induced salinity and acidic pH conditions [J]. Chemosphere, 2016, 142: 64-71. https://doi.org/10.1016/j.chemosphere.2015.06.079

[34] YANG G-X, JIANG H. Amino modification of biochar for enhanced adsorption of copper ions from synthetic wastewater [J]. Water Research, 2014, 48: 396-405.https://doi.org/10.1016/j.watres.2013.09.050

[35] SONG J, HE Q, HU X, et al. Highly efficient removal of Cr(VI) and Cu(II) by biochar derived from Artemisia argyi stem [J]. Environ Sci Pollut Res Int, 2019, 26(13): 13221-13234. https://doi.org/10.1007/s11356-019-04863-2

[36] IDREES M, BATOOL S, KALSOOM T, et al. Animal manure-derived biochars produced via fast pyrolysis for the removal of divalent copper from aqueous media [J]. Journal of Environmental Management, 2018, 213: 109-118. https://doi.org/10.1016/j.jenvman.2018.02.003

[37] KOŁODYŃSKA D, WNĘTRZAK R, LEAHY J J, et al. Kinetic and adsorptive characterization of biochar in metal ions removal [J]. Chemical Engineering Journal, 2012, 197: 295-305. https://doi.org/10.1016/j.cej.2012.05.025

Biography

Tao Tao Sun graduated with a Bachelor's Degree from the School of Environment, China University of Geosciences in July 2022 and is currently enrolled in Anhui Polytechnic University to pursue a Master's Degree.

Mian Muhammad Ahson Aslam is a postdoctoral researcher with a PhD in Environmental Science and Engineering. He earned his bachelor's and master's degrees from Bahauddin Zakriya University, Pakistan, and his PhD from Tunghai University, Taiwan, where he received the Phi-Tau-Phi Scholastic Award. Since November 2023, Dr. Aslam has been affiliated with Anhui Polytechnic University, China. He has held academic and research positions at Bahauddin Zakriya University, Pakistan; Tunghai University, Taiwan; Texas A&M University, USA; and GeoNano Environmental Tech, Taiwan. Additionally, he has collaborated with Hamburg University of Technology, Germany, and Hamad Bin Khalifa University, Qatar. Dr. Aslam has authored several SCI papers and international conference papers, and contributed to book chapters published by Elsevier. He recently secured a research project on "Enhanced Remediation of Coastal Saline Soil Using Biochar-Based Composite Materials" from the Ministry of Natural Resources, China, where he serves as the principal investigator.

Guangquan Chen received his PhD degree in Estuarine Coastal Science from the State Key Laboratory of Estuarine Coastal Science, East China Normal University. He is a visiting scholar of Department of Marin Chemistry and Geochemistry, Woods Hole Oceanographic Institution, USA.

Yuchen Ye graduated from Sichuan Agricultural University with a bachelor's degree in 2023 and is currently studying for a master's degree in the College of Chemical and Environmental Engineering at Anhui Polytechnic University.

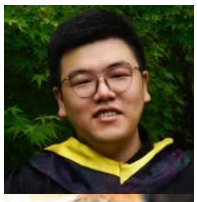

Wentao Xu graduated from Anhui Polytechnic University in August 2022 with a Bachelor's Degree and is studying for a Master's Degree in the College of Chemical and Environmental Engineering at Anhui Polytechnic University.

Changsheng Peng, selected by the Ministry of Education's New Century Outstanding Talents Support Program, graduated from Anhui University of Science and Technology (B.S.) in July 1993, M.S. from China University of Mining and Technology (M. M. T. U.) in July 1996, Ph.D. from University of Science and Technology Beijing (USTB) in March 2003. 2005-2021, Ocean University of China, 2022-present, Anhui University of Engineering. He has been awarded the Second Prize of "New Century Outstanding Talents" by Ministry of Education (2008), the Second Prize of "Tiantai Outstanding Talents" by Qingdao (2009), the Advanced Individual of Nansihu Water Specialization in Shandong Province (2013), and the Second Prize of Science and Technology Progress in Qingdao (2023). He has presided over and participated in 6 national projects, 7 provincial and ministerial projects, 8 other vertical and horizontal projects, with a funding of more than 5 million yuan, published more than 200 academic papers, with a total of more than 10,000 citations, h-factor of 42, and authorized more than 10 patents; published a book, written chapters for 3 monographs, and many papers for ESI high citation or hot paper; invited guest of "Into the Deep Blue", a science and technology program of Shandong Television Station. He has been invited as a special guest of Shandong TV's science and technology program "Into the Deep Blue".

Research Field

TaoTao Sun: Biochar synthesis and modification for environmental remediation, Co-Pyrolysis of biomass and red mud for iron extraction

Mian Muhammad Ahson Aslam: Biochar synthesis and modification for costal soil remediation, Co-Pyrolysis of biomass and red mud for iron extraction, Adsorbents preparation and environmental applications, Adsorption technology in wastewater treatment (heavy metals uptake), Degradation of total petroleum hydrocarbon (TPH)-related pollutants (e.g., MTBE, BTEX) and some solvents (e.g., PCE, TCE)

Guangquan Chen: Mechanism of groundwater radium-radon isotope transport during seawater intrusion and its indication of seawater intrusion. Research and development of multi-parameter in situ monitoring technology for seawater intrusion and soil salinization based on Internet of Things technology. Prediction of seawater intrusion trend based on deep learning model. Research on the prevention and control technology of seawater intrusion and soil salinization.

Yuchen Ye: Biomass Resource Treatment. Preparation and application of biochar.

Wentao Xu: Sludge separation research and equipment development.

Changsheng Peng: Environmental materials and environmental protection equipment, soil and groundwater pollution remediation, sea (salty) water desalination and resource utilization.